Eur. Phys. J. D **45**, 129–132 (2007)
DOI: 10.1140/epjd/e2007-00153-2

THE EUROPEAN PHYSICAL JOURNAL D

Preparing a laser cooled plasma for stopping highly charged ions

M. Bussmann[a], U. Schramm, and D. Habs

Ludwig-Maximilians-Universität München, Department für Physik, Am Coulombwall 1, 85748 Garching, Germany

Received 25 January 2007
Published online 11 May 2007 –

Abstract. We present a new cooling scheme for the preparation of highly charged ions for future in-trap precision experiments. A plasma of laser cooled $^{24}Mg^+$ ions trapped in a 3D harmonic confinement potential is used as a stopping medium for the highly charged ions. We focus on the dynamic evolution of the plasma, determining suitable cooling conditions for fast recooling of the $^{24}Mg^+$ ions. The results of a realistic parallel simulation of the complete stopping process presented here indicate that a small, constant detuning of the laser frequency is sufficient for subsequent recooling of the plasma, thus maintaining the stability of the plasma.

PACS. 02.70.Ns Molecular dynamics and particle methods – 32.80.Pj Optical cooling of atoms; trapping – 34.50.Bw Energy loss and stopping power – 52.27.Gr Strongly-coupled plasmas

1 Introduction

The preparation of cold highly charged ions is a vital prerequisite for future in-trap precision experiments [1–4]. High charge states allow to gain precision for example in determining nuclear masses or measuring QED effects with tightly bound electrons.

2 Using a laser cooled plasma as a stopping medium

We present a new scheme for in-trap preparation of ultra cold highly charged ions using a laser cooled one component plasma of $^{24}Mg^+$ ions as a stopping medium. In the following we focus on the cooling conditions necessary to maintain a stable $^{24}Mg^+$ plasma and investigate possible charge exchange processes which could reduce the high charge state of the ion of interest.

Laser cooling is a common tool to create ultra cold atomic or ionic ensembles in a very short time [5]. Here we concentrate on in-trap laser cooling of ions, which at present can provide large ensembles of 10^5 to 10^6 ions at temperatures of only a few mK. Laser cooling exploits the strong force a laser beams exerts on the ion when the laser frequency is in resonance with the cooling transition of interest. Only a few ion species provide a closed ground transition suitable for cooling and thus the majority of ion species cannot be directly laser cooled. This limitation can be overcome when considering the Coulomb interaction of the ion of interest with laser cooled ions.

[a] e-mail: michael.bussmann@physik.uni-muenchen.de

In a laser cooled plasma the mutual Coulomb interaction transfers energy from the hot, highly charged ion which is not laser cooled to the laser cooled ions. If the velocity of the laser cooled ions is kept in the acceptance range of the laser force during this heating process, fast recooling is possible — thus maintaining the plasma characteristics during the cooling.

It is important to note that the transfer of energy per interaction increases linearly with the charge state of the ion of interest. Thus the cooling rate increases with the ion charge state. In modern trap setups such as Penning or Paul traps an ensemble of laser cooled ions of charge state Q can undergo a phase transition into a crystalline state [5–7]. In this state the ion positions are frozen out, because the mutual Coulomb repulsion has overcome the kinetic energy of the ions by orders of magnitude. The plasma of density n and temperature T is strongly coupled, meaning that the plasma parameter $\Gamma = (Q^2e^2)/(4\pi\epsilon_0 k_B T a_{\mathrm{WS}})$ exceeds unity.

External confinement forces counteract the mutual repulsion of the ions, thereby determining the form and structure of the Coulomb crystal. In a harmonic trap potential the ion crystal resembles a prolate ellipsoid of length L_{axial} and width L_{radial} while the ions are ordered at an equal spacing of $a_{\mathrm{WS}} = (3/4\pi n_{\mathrm{Mg}})^{1/3}$, the Wigner-Seitz radius. In the simulation presented a single highly charged ion is placed near the brim of the ellipsoid, its velocity vector pointing towards the plasma's center, see Figure 1. The axial confinement Ψ_{axial} is much weaker than the radial confinement Ψ_{radial}. In such a configuration the density of the plasma is mainly determined by the radial confinement, while the large axial extent of

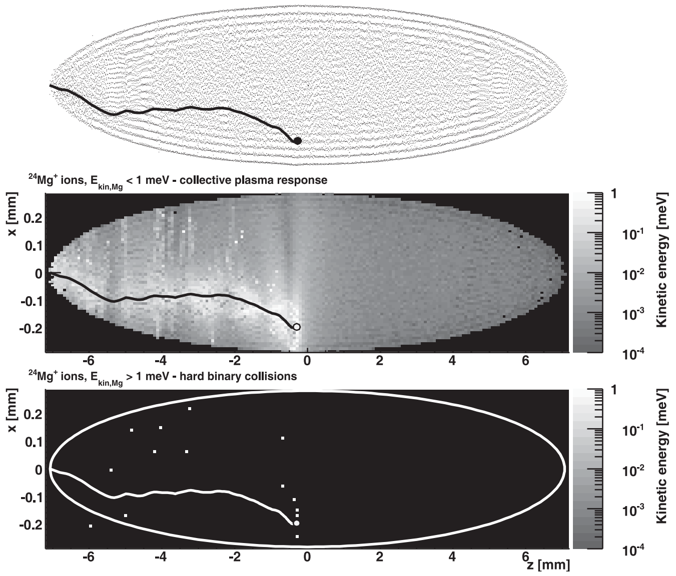

Fig. 1. Three different views of a $^{24}\mathrm{Mg}^+$ plasma ellipsoid of density $n_{\mathrm{Mg}} = 4.23 \times 10^{13}$ m^{-3}, 11.1 μs after a highly charged ion with an initial energy $E_{\mathrm{kin,HCI}} = 400$ meV and charge state $Q_{\mathrm{HCI}} = 40$ has entered the plasma. At this point in time all the kinetic energy of the heavy ion has been deposited in the plasma. The upper part shows a real space image of a vertical slice through the center of the plasma ellipsoid, including the path of the heavy ion and its current position marked by a circle. The two lower parts show an intensity-coded distribution of the kinetic energies of the $^{24}\mathrm{Mg}^+$ ions, integrated in y-direction.

the plasma allows for many subsequent interactions of the highly charged ion with the plasma ions.

3 Characterizing the stopping process. A realistic molecular dynamics simulation of the plasma-plasma and plasma-HCI interaction

Although standard stopping theory [8] can provide an estimate of the overall stopping power for a highly charged ion of given charge state Q_{HCI} and initial energy $E_{\mathrm{kin,HCI}}$, it does not provide insight into the dynamics of the stopping process.

In the special case of the strongly coupled plasma studied here, the response of the ions when interacting with the highly charged ion cannot be treated assuming a simple binary collision model. Instead, the evolution of the plasma during the stopping process must include a realistic description of the coupling between the ions.

We introduce a newly developed simulation which completely integrates strong coupling into the stopping process by computing the Coulomb interaction between all particles involved. This ansatz requires efficient parallel algorithms since the computation effort essentially scales with the square of the number N of interacting particles considered.

The equation of motion

$$m_i \frac{d^2\mathbf{r}_i}{d^2t} = \left(\sum_{j\neq i}^{N+1} \frac{q_i q_j}{4\pi\epsilon_0 |\mathbf{r}_i - \mathbf{r}_j|^3} (\mathbf{r}_i - \mathbf{r}_j) \right) - q_i \left(\Psi_{\mathrm{radial}}, \Psi_{\mathrm{radial}}, \Psi_{\mathrm{axial}}\right) \begin{pmatrix} x_i \\ y_i \\ z_i \end{pmatrix} + F_{\mathrm{laser}} \left(\frac{d\mathbf{r}_i}{dt} \right) \tag{1}$$

is solved for each particle i of the $N+1$ simulated particles at position $\mathbf{r}_i = (x_i, y_i, z_i)$.

With this high number of particles a realistic model of the real stopping process can be studied without relying on quasi-particle models. In the equation of motion the laser force can be approximated by an effective force depending only on the ion velocity $\mathbf{v}_i$:

$$F_{\mathrm{laser}}(\mathbf{v}_i) = \frac{\hbar}{8} \frac{S \Gamma_{\mathrm{laser}}^3 \mathbf{k}_{\mathrm{laser}}}{(\delta - \mathbf{v}_i \cdot \mathbf{k}_{\mathrm{laser}})^2 + (\Gamma_{\mathrm{trans}}/2)^2 (1+S)} \tag{2}$$

where the laser beam is characterized by the saturation parameter S and the wave vector $\mathbf{k}_{\mathrm{laser}} = (0, 0, \pm 2\pi/\lambda_{\mathrm{laser}})$. Cooling $^{24}\mathrm{Mg}^+$ ions requires a laser wavelength of $\lambda_{\mathrm{laser}} =$ 280 nm.

In a typical cooling setup two laser beams are applied from opposite directions along the axial direction at a small detuning δ of the laser frequency relative to the frequency of the cooling transition. In such as set-up the momentum acceptance of the laser force is on the order of the transition line width Γ_{trans} ($\Gamma_{\mathrm{trans}} = 2\pi \times 42.7$ MHz for $^{24}\mathrm{Mg}^+$). Fast recooling is only possible if the majority of the ions can be addressed by the laser force choosing a fixed detuning δ.

In the study presented here the laser force is deliberately set to $F_{\mathrm{laser}} \equiv 0$ in order to study the unperturbed evolution of the velocity distribution of the plasma during the passage of the HCI through the plasma. The simulation thus allows to study the plasma dynamics of the precooled crystalline ensemble of ions during the stopping process in order to optimize the final laser parameters for efficient recooling of the laser ions.

In the special case considered, $N = 10^5$ laser cooled $^{24}\mathrm{Mg}^+$ ions are introduced as a stopping medium for one highly charged ion (HCI) of mass $m_{\mathrm{HCI}} = 100$ a.m.u. The initial kinetic energy $E_{\mathrm{kin,HCI}}$ and the charge state Q_{HCI} of the HCI as well as the density n_{Mg} of the plasma have been varied to study their influence on the stopping process. All the relevant simulation parameters are found in Table 1.

4 Binary collisions vs. collective plasma response

The interaction of the HCI and the plasma ions can be separated in two parts: at small impact parameters b the interaction is governed by close binary collisions, while at large impact parameters the energy is transferred into a collective response of a major part of the plasma, each

Table 1. Parameters for the simulation.

Simulation input parameters		
integration time $\Delta\tau_{\text{step}}$ [s]	10^{-9}	
Ψ_{radial} [V/m^2]	2.5×10^5	3.5×10^5
Ψ_{axial} [V/m^2]	2.5×10^3	3.5×10^3
Plasma input parameters		
Number of Mg^+ ions	10^5	
$A_{\text{Mg}}, Q_{\text{Mg}}$	$24, 1$	
T_{Mg} [K]	10^{-3}	
HCI input parameters		
Number of highly charged ions	1	
A_{HCI}	100	
Q_{HCI}	$10, 20, 30, 40$	
$E_{\text{kin,HCI}}$ [meV]	$100, 200, 300, 400$	
Plasma properties derived from the simulation		
Γ_{Mg}	814	911
$a_{\text{WS}}(n_{\text{Mg}})$ [m]	19.9×10^{-6}	17.8×10^{-6}
L_{radial} [m]	632×10^{-6}	565×10^{-6}
L_{axial} [m]	15.8×10^{-3}	14.1×10^{-3}
n_{Mg} [m^{-3}]	3.02×10^{13}	4.23×10^{13}

of the plasma ions carrying only a small fraction of the energy.

Following the argument given in [9] one can estimate that those $^{24}Mg^+$ ions with a kinetic energy $E_{\text{kin,Mg}} > 1$ meV took part in a close binary collision with the HCI. Figure 1 shows three views of the HCI's trajectory inside the plasma to illustrate this differentiation. At the start of the simulation the HCI is placed on axis near the brim of the plasma ellipsoid and is then given its initial kinetic energy, its velocity vector pointing to the center of the plasma ellipsoid.

The upper part of Figure 1 shows a slice through the center of the $^{24}Mg^+$ ensemble revealing the crystalline shell structure with the solid line following the trajectory of the HCI and the filled circle marking its position. For the same set of simulation parameters the middle part and lower part show the spatial distribution of the kinetic energy of the $^{24}Mg^+$ ions, again including the HCI trajectory and position. The middle part shows the distribution of the kinetic energy for all $^{24}Mg^+$ ions with $E_{\text{kin,Mg}} < 1$ meV while in the lower part only those few ions with $E_{\text{kin,Mg}} > 1$ meV enter the plotted distribution. The logarithmic scale chosen for the intensity-encoded kinetic energy reveals the large extent of the plasma region affected by the passage of the HCI. The corresponding simulation parameters are $n_{\text{Mg}} = 4.23 \times 10^{13}$ m^{-3}, $E_{\text{kin,HCI}} = 400$ meV and $Q_{\text{HCI}} = 40$.

5 Charge exchange, plasma stability and fast recooling

As can be deduced from Figure 1 the number of $^{24}Mg^+$ ions carrying a large kinetic energy after a close collision with the HCI is minute compared to the total number of ions in the plasma. Furthermore, the crystalline structure is not destroyed by the HCI. Nevertheless, the amount of energy carried away by those few ions is of the same order as the energy deposited in the bulk of the plasma, as shown in the right part of Figure 2, where the total kinetic energy E_{high} of all ions with $E_{\text{kin,Mg}} > 1$ meV is compared to the total kinetic energy E_{low} of all ions with $E_{\text{kin,Mg}} < 1$ meV.

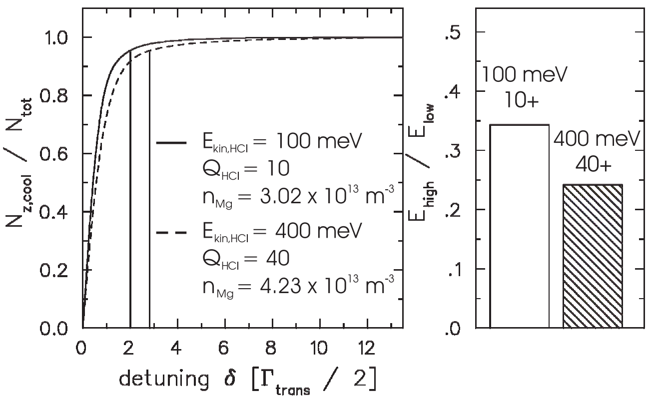

Fig. 2. Left: ratio of the number $N_{\text{z,cool}}$ of ions with $v_{\text{z,Mg}} \leq v_\delta$ and the total number $N_{\text{tot}} = 10^5$ of $^{24}Mg^+$ ions versus the laser detuning in units of transition line width $\Gamma_{\text{trans}}/2$. The vertical lines mark the detuning value at which 95.4% of the ions are within the acceptance of the laser force. Right: sum E_{high} of the kinetic energy for all ions with $E_{\text{kin,Mg}} > 1$ meV over the sum E_{low} of the kinetic energy for all ions with $E_{\text{kin,Mg}} < 1$ meV. The hollow box corresponds to the same data set as the solid line in the left part, the hatched box to the dashed line.

Following equation (2) one can choose a fixed detuning δ matched to the range of $^{24}Mg^+$ ion velocities in order to recool almost all $^{24}Mg^+$ ions without scanning the laser frequency. The choice for δ also depends on the individual trap characteristics which manifest in a heating rate intrinsic to the trap system which must be counteracted by the cooling laser force [10]. This heating rate becomes more important for large crystals which ultimately limits the value of the detuning δ to a few times the natural transition line width.

Fortunately, the simulation results show that this constraint can be met without significant ion loss. Depending on the desired percentage of ions which should be directly addressed by the laser force one can reduce the detuning, thus increasing the cooling rate for the majority of the $^{24}Mg^+$ ions. This is illustrated in Figure 2 where the percentage of ions with $v_{\text{z,Mg}} \leq v_\delta$ is plotted versus the detuning $\delta = \mathbf{v}_\delta \cdot \mathbf{k}_{\text{laser}}$. Here, two different scenarios are compared, one in which the total energy deposited in the plasma and the energy loss $dE_{\text{kin,HCI}}/ds$ are small (solid line) and one case for which both values are higher in comparison (dashed line). For both curves the majority of the ions can be easily cooled using only a small laser detuning. Thus we conclude that small detuning values are feasible for recooling. It is therefore not necessary to constantly detune the laser frequency, which must be performed on the order of seconds to efficiently reduce a large momentum spread of the ion ensemble. Instead, a laser beam with a moderate saturation parameter S on the order of unity and a fixed laser frequency are sufficient to recool the ensemble on a time scale of few ms [5] comparable

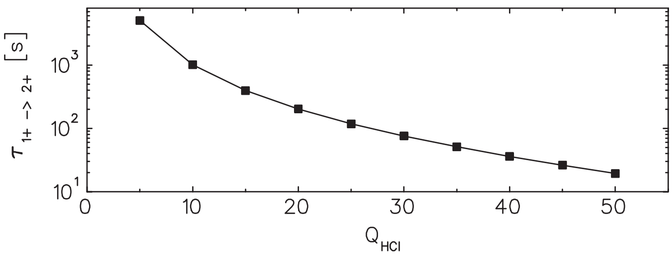

Fig. 3. Average time $\tau_{1+\to 2+}$ for the charge exchange process $^{100}X^{Q+} + {}^{24}Mg^{1+} \to {}^{100}X^{(Q-1)+} + {}^{24}Mg^{2+}$ for a HCI X with energy $E_{\mathrm{kin,HCI}} = 400$ eV at a plasma density of $n_{\mathrm{Mg}} = 4.23 \times 10^{13}$ m^{-3}.

to the total stopping time [9], reaching repetition rates of kHz.

Charge exchange becomes important especially for the high charge states demanded by future precision experiments. Experimental data [11,12] still is rare for charge exchange processes with highly charged ions at small relative velocities. Thus one has to rely on theoretical models of charge exchange [13] to give an estimate on the cross sections and exchange rates expected in a typical cooling setup as shown in Figure 3. The figure shows an estimate for an initial kinetic energy of $E_{\mathrm{kin,HCI}} = 400$ eV, a factor 1000 higher than the energies used in the simulation, thereby clearly showing that charge exchange can be neglected in the cooling scheme proposed here.

6 Summary

We have introduced a new cooling scheme using laser cooled ions to efficiently cool highly charged ions. Ion losses due to charge exchange are negligible while fast recooling is possible. Highly charged ions can be cooled to mK temperatures, either for later extraction or integration into the Coulomb crystal lattice after recooling. After the stopping of the highly charged ion the plasma can be recooled fast, without detuning of the laser frequency or reloading of ions to the trap.

References

1. J. Dilling et al., Int. J. Mass Spectrom. **251**, 198 (2006)
2. F. Herfurth et al., Int. J. Mass Spectrom. **251**, 266 (2006)
3. R. Ringle et al., Int. J. Mass Spectrom. **251**, 300 (2006)
4. D. Habs et al., Eur. Phys. J. A **25**, 57 (2005)
5. U. Schramm, D. Habs, Prog. Part. Nucl. Phys. **53**, 583 (2004), and references therein
6. D.J. Wineland et al., Phys. Rev. Lett. **59**, 2935 (1987)
7. H. Walther, Adv. At. Mol. Opt. Phys. **31**, 137 (1993)
8. G. Zwicknagel et al., Phys. Rep. **309**, 117 (1999)
9. M. Bussmann et al., Proceedings of the International Workshop on Non-Neutral Plasmas NNP06, Aarhus, 2006, edited by M. Drewsen (AIP Conf. Proceedings **862**, Melville, 2006), p. 221
10. U. Schramm et al., J. Phys. B **36**, 561 (2003)
11. H. Cederquist et al., Phys. Rev. A **51**, 2191 (1995)
12. B.R. Beck et al., Phys. Rev. Lett. **77**, 1735 (1996)
13. R.E. Olson et al., Phys. Rev. A **14**, 579 (1976)